ENERGY HARVESTING BY MEANS OF STIFFNESS VARIABLE SPRING DEVICE

Patrick Scholle, p.scholle@tu-braunschweig.de, TU Braunschweig (Germany)

Fred Nitzsche, fred-nitzsche@carleton.ca, Carleton University (Canada)

Wander Vieira, wander.vieira@usp.br, University of Sao Paulo (Brazil)

Michael Sinapius, m.sinapius@tu-braunschweig.de, TU Braunschweig (Germany)

Abstract

In this paper, an electro-mechanical system based on the "smart spring" concept is analyzed [1]. The "smart spring" existing stiffness control capabilities for rotorcraft vibration attenuation are extended to work as an energy harvesting device. The device is targeted to supplement or potentially replace the conventional lead-lag damper in helicopters. It is designed to provide the necessary attenuation for the lead-lag blade mode and, simultaneously, harvest electrical energy inside the rotating frame. The „smart spring" concept consists of two load paths, each represented by a mechanical spring. The secondary load path includes a damping element and a piezoelectric actuator, as indicated in Figure 1. The basic principle of the concept is to allow the secondary load path to engage and disengage through a friction-based mechanism actuated by a piezoelectric element. In the present work, a control principle based on an analogy between the „smart spring" and the control algorithm known as *Synchronized Switch Damping on Inductor (SSDI)* is analyzed throughout numerical simulations [2]. The results indicate the possibility to generate large damping forces when the SSDI control algorithm is used in the „smart spring". An optimized „smart spring" design is then integrated into a simple 1 Degree of Freedom (DOF) model of the lead lag damper of a helicopter to provide an additional damping element to the conventional device. Simulations that use the „smart spring" damper as an supplementary damping element, thus supplying only 8% of the total damping, show that a mean power of up to 10 W can be harvested in the 130 kn forward flight condition. The maximum power of the presented device is currently limited by a pre-set maximum clamping force of the friction based clamping of the "smart spring". The „smart spring" energy harvester would potentially be integrated into a multi-functional device that replaces the lead lag damper element, producing peak mean power outputs of up to 100 W per blade.

1. MOTIVATION

Fully articulated helicopter blades have three hinges. While the flapping motion is damped sufficiently through aerodynamic effects, the lagging motion is not. Thus arise two dangerous phenomena called air and ground resonance that have to be resolved by adding damping to the lead lag motion. Many commercial helicopters resolve this problem by adding damping elements to each blade that dissipate the kinetic energy of the lead-lag motion and

thereby stabilize the system. The main idea for this work is to transduce all or part of this kinetic energy into useful electric energy instead of dissipating it. Ultimately this is supposed to lead to a multifunctional device that generates a stable power supply directly inside the rotating frame of the helicopter. Current helicopter designs that require power in the rotating frame use slip rings that transmit electrical energy from the main body to the rotating frame. This type of connection has to be maintained regularly and the helicopter would, therefore, benefit from the

establishment of a robust power source directly in the rotating frame. The energy in the rotating frame can be used for a variety of applications.

One example of such application is a Structural Health Monitoring (SHM) system. Helicopter blades are currently being replaced after a relatively short lifetime. Since the structural integrity of the blades has to be flawless at all times in order to guarantee a safe flight, the lifetime calculations assume absolute worst case scenarios. Thus, blades are being discarded that would otherwise be capable of many more flight hours. A SHM system can expand the usage time in these cases by constantly monitoring the structural integrity of the blade and thus giving the ability to only replace a blade when it is necessary. Another device that would require energy in the rotating frame is the Active Pitch Link (APL) developed by the Rotorcraft Research Group at Carleton University [1]. Conventional pitch links are designed as rigid links. Vibrations, excited by turbulent airflow at the blades are thus directly transmitted to the main body of the helicopter. This is a major source of noise and riding discomfort for the passengers. The proposed APL was designed to overcome these problems by altering the structural impedance at the blade root. Experimental tests showed the effectiveness of the APL and, furthermore, proofed that the device does not influence other important rotordynamic characteristics, especially the fundamental 1/rev rotor cyclic control.

2. CURRENT RESEARCH WORKING ON THE „SMART SPRING" PROJECT
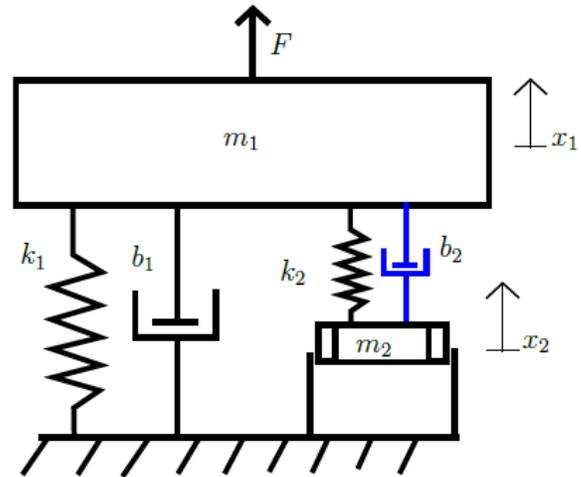
Figure 1: General Idea of the „smart spring" concept with the main load path (m_1, b_1, k_1) and the secondary load path (m_2, b_2, k_2), which is able to engage and disengage to the ground using a piezoelectric clamping mechanism.

Figure 1 shows a schematic view of the „smart spring" concept. The „smart spring" is made up of two mass-spring-damper systems. While one of those systems is connected directly to the ground (the swashplate), the second system is connected to a piezoelectric stack actuator. The stack can expand in horizontal direction and create a friction force with the sleeves by applying a voltage. If the friction force is sufficiently high, the secondary system can be locked to the ground. In recent work, Nitzsche and Vieira et al. [3] [4], describe an interesting analogy between the „smart spring" and a group of control laws developed by Richards et al [2]. The former authors realized that a stiffness variable structure as depicted in Figure 1 is indeed the mechanical representation of the SSDI control system developed by Richard et al. In the SSDI analogy, the electrical resonant circuit is represented by the mechanical secondary system. The piezo voltage is represented by the force that the spring k_2 exerts on the mass m_1. Vieira et al. showed the

working principle of the SSDI controlled „smart spring" with numerical studies and got promising results for reducing vibration .

3. DEVELOPMENT OF AN ANALYTICAL MODEL OF THE „SMART SPRING" USING AN EQUIVALENT VISCOUS DAMPING APPROACH

The basic idea of the SSDI control is to switch the secondary system in a synchronous way with the main vibration system. When applied to the „smart spring", this control leads to a system

spring. At state 2, the kinetic energy of the main mass is almost zero. When the kinetic energy of the main mass reaches zero after this state, the secondary load path triggers the inversion process as described by the SSDI control law. Thus, the main mass is still at the same position at state 3, but the second mass traveled upwards and is now no longer prestressed with a tensile force but with a compression force. Therefore, the potential energy of the spring increases again when the main mass travels down subsequently. After a second inversion process between state 4 and 5, the cycle is once
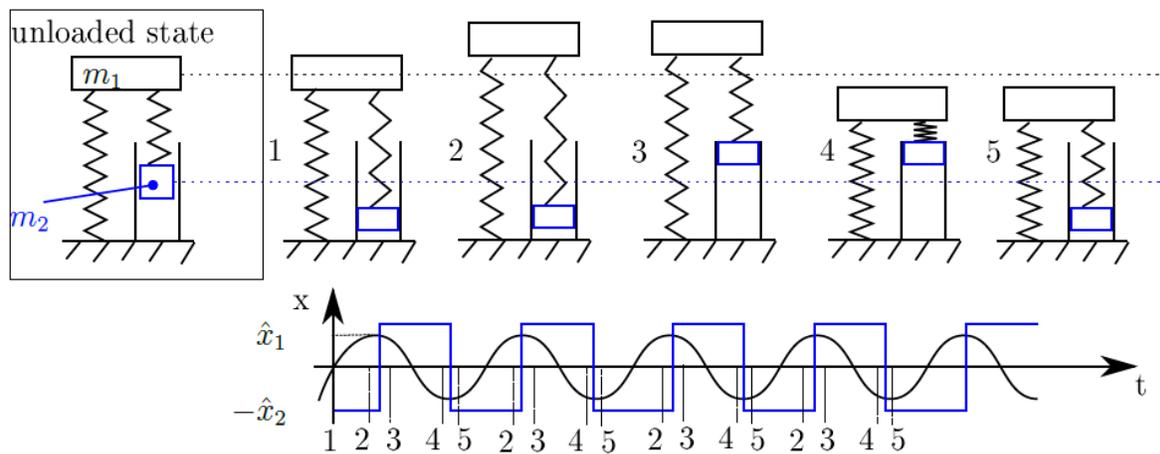
Figure 2: Principle movement of a SSDI analogous controlled smart spring under force excitation of the main mass.

where the secondary load path is engaged for most of the time. Whenever the velocity of the main load path reaches zero, the secondary load path is released for a brief timelength, the duration of which is equal to one half of it's eigenfrequency. Figure 2 shows the system behavior of a force excited „smart spring" with a SSDI analogous control design. The main mass performs harmonic vibration with an amplitude of $\hat{x}_1$ while the second mass performs a square wave type of oscillation with the maximum displacement $\hat{x}_2$. The Figure, furthermore, shows 5 discrete system states in a schematic way. At state 1, the main mass moves upward and thereby elongates both main and secondary

more at it's beginning and the cycle repeats itself. It should be noted, that the secondary spring never increases the kinetic energy of the main mass due to the inversion of displacement. In other words, the secondary spring force always acts against the movement of the main mass. The spring force can therefore be interpreted as a damping force for the main mass. However, the damping effect is produced purely by non-dissipative elements – a switching mass-spring system. For this reason the "smart spring" has beed categorized as a *stiffness control* element. In this paper, this damping is referred to as *induced* damping in order to differentiate it from the damping that originates

from the physical damping elements. This is a very important working principle for the amplitude reduction of the „smart spring" secondary mass. When the spring k_2 is getting elongated or compressed, energy is being stored in form of potential energy. Since the spring gets once elongated and once compressed in each period, the energy transferred to the secondary spring system each cycle can be calculated with:

(1) $W_{d,i} = 2 \int\limits_{\hat{x}_2-\hat{x}_1}^{\hat{x}_2+\hat{x}_1} k_2 x \, dx = 4k_2\hat{x}_1\hat{x}_2 = 4k_2\hat{x}_1^2\alpha$

where α is the ratio of amplitudes of main and secondary load pathes in steady state and k_2 is the stiffness of the secondary load path.

In order to quantify this induced damping, an equivalent viscous damping approach is used in this paper. In this approach, an equivalent damping constant b_{eqv} is defined in a way, that the dissipated energy per period of the induced damping is identical to that of a regular viscous damper. The energy dissipated in one cycle T of the steady state condition of any system with velocity proportional damping can be determined by:

(2) $W_d = \int\limits_0^T F_d dx = \int\limits_0^T b\dot{x}dx = \int\limits_0^T b\dot{x}^2 dt$

Using the assumption of harmonic motion $x(t) = \hat{x}\sin(\omega t - \varphi)$, equation (2) can be solved to:

(3) $W_d = b\omega^2\hat{x}^2 \int\limits_0^{2\pi/\omega} \cos^2(\omega t - \varphi)dt = \pi b\omega\hat{x}^2$

This equation can be rearranged to define the equivalent damping constant:

(4) $b_{eqv} = \dfrac{W_d}{\pi\omega\hat{x}^2}$

Combining equation (4) and (1), the equivalent damping constant of the SSDI analogous controlled „smart spring" can be defined as:

(5) $b_{eqv} = \dfrac{4k_2\alpha}{\pi\omega}$

In order to further develop this equation, an equation for the amplitude ratio α has to be found. In steady state, the amplitude of the secondary load path is constrained by the damper b_2 as displayed in Figure 1. For the following calculations, it is assumed that the inversion of the secondary load path takes place very fast when compared to the period time of the main load path. With this assumption, the main load path can be assumed to be stationary in space during the inversion of the second mass. The movement of the secondary mass during the inversion can then be described by the equations governing a simply viscously damped 1 DOF system subjected to an initial displacement. The decay curve of a viscously damped system can be found in the basic vibration analysis literature:

(6) $x(t) = \hat{x}e^{-\zeta\omega_0 t}\cos(\omega_d t), 0 < \zeta < 1$

where ζ is the damping rate of the system, ω_0 is the eigenfrequency of the undamped system, and ω_d is the eigenfrequency of the damped system. As defined by the SSDI control, the mass performs one half oscillation before it is clamped again. The amplitude after the inversion can then be calculated as $x(\frac{T}{2})$. Revisiting Figure 2, it can be observed that the secondary spring has a displacement equal to $\hat{x}_1 + \hat{x}_2$ before the inversion. $\hat{x}_2$ can then be described in steady state as the sum of $\hat{x}_1$ and whatever amplitude that remains after one half oscillation of the secondary load path with an initial displacement of $\hat{x}_1 + \hat{x}_2$:

(7) $\hat{x}_2 = \hat{x}_1 + (\hat{x}_1 + \hat{x}_2)e^{-\zeta_2\frac{\pi}{\sqrt{1-\zeta_2^2}}}$

Reorganizing this equation, an analytical expression for the amplitude ratio α may be found:

$$(8) \quad \frac{\hat{x}_2}{\hat{x}_1} = -\coth\left(\frac{-\zeta_2\pi}{2\sqrt{1-\zeta_2^2}}\right) := \alpha$$
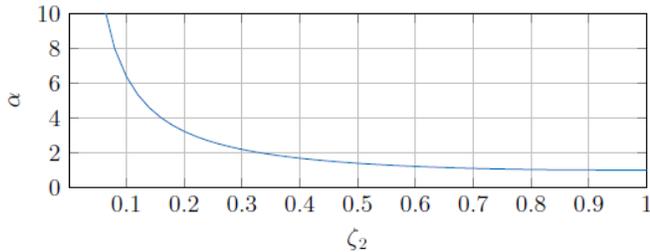
Figure 3: Amplitude ratio for various damping rates of the secondary load path.

Figure 3 shows the progression of the amplitude ratio for damping rates between 0 and 1. The plot demonstrates how the damping in the secondary load path limits the amplitude of the same, because the amplitude ratio grows quickly for damping rates smaller than 0.1.

Combining equations (4) and (8) allows to easily estimate the system behavior of a „smart spring" system displayed in Figure 1. The system can be significantly simplified to a 1 DOF model by applying the described equivalent damping approach. Figure 4 shows the simplified model, where the influence of the induced damping of the secondary load path with SSDI analogous control is now included as the equivalent damping b_{eqv}. The approach is validated by comparing the system behavior of a numerical model based on Figure 1 to that of the model with equivalent damping displayed in Figure 4.
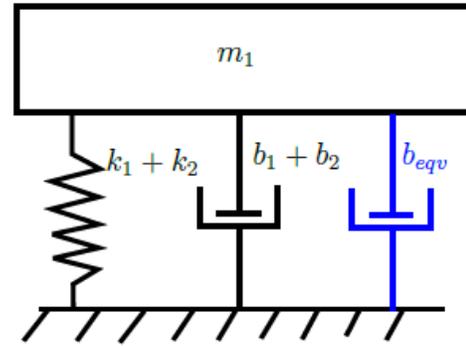
Figure 4: Simplified model of the „smart spring" with the equivalent damping approach

The benefit of using the „smart spring" for inducing damping to a mechanical system instead of using a regular damping element directly becomes apparent, when the magnitude of the equivalent damping factor is calculated and compared to the physical damping build into the system. *Keeping in mind that the equivalent damping does not originate from a physical damping element but from a spring-mass system it becomes clear that all energy dissipation still has to take place using the physical damping elements.* In the previous successful experimental demonstrations of the "smart spring" system, dissipation of energy occurred totally in the clamping (frictional) mechanism. However, simulations show, that most of the energy dissipation may take place in a damper build into the secondary load path. The equivalent damping factor induced by the „smart spring" can be orders of magnitude larger than that provided by the latter physical damping elements built into the secondary load path. The overall damping factor is, therefore, amplified through the SSDI controlled „smart spring".
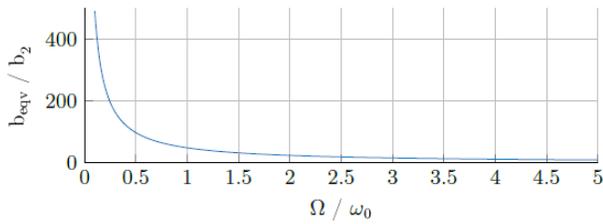
Figure 5: Amplification of the damping factor through the application of the „smart spring" damping idea. $\xi_2 = 0.3$

Figure 5 shows the amplification of damping for various excitation frequencies. It can be observed, that the „smart spring" is especially effective for low-frequency applications, where the *excitation frequency is smaller than the eigenfrequency of the system*. For this reason, it's inventors called the smart spring a stiffness-controlled device (as opposed to damping-controlled or mass-controlled device – where the excitation frequency is equal or greater the eigenfrequency of the system, respectively). Since the force used for damping does not originate from a velocity-proportional damper but from a mechanical spring, comparatively high control forces can be achieved for comparably low velocities – an especially useful design for controlling rotorcraft blades vibrations.

The amplification of the damping constant can be exploited for the purpose of *energy harvesting*. When an electromagnetic damper is built into the secondary load path, a comparably small but efficient electro-mechanical coupling can be generated that induces, in addition, large damping rates to the system. Indeed, previous studies showed, that electromagnetic dampers do not offer both large damping forces and a high energy conversion efficiency [5]. This dilemma could be overcome by using the „smart spring" damping approach.

4. BRIEF INTRODUCTION TO ELECTROMAGNETIC DAMPERS

In this chapter, a brief overview of the working principles of electromagnetic dampers is presented. Please refer to the literature for more elaborate explanations [5] [6] [7].

Electromagnetic energy harvesting is based on the principle of electromagnetic induction discovered by Michael Faraday in 1831. When a conductor moves perpendicular to a constant magnetic field at a constant velocity, the generated electrical eddy field induces a voltage in the conductor:

(9) $U_{emf} = Bvl_w$

Where B is the magnetic flux density, v is the velocity and l_w is the length of the inductor. When an electromagnetic damper gets connected to a circuit, a current flows due to this induced voltage. Spreemann et al. [8] describe in their book on electromagnetic energy harvesting, how this current then forms a magnetic field, which opposes the movement of the conductor. Thus, this electro-mechanical coupling can be used as a mechanical damper. In order to maximize the length of the inductor, it is often times implemented as a coil in practical solutions. Zuo and Zhang present a feasible solution how coils and magnets can be arranged to construct an electromagnetic damper [5] [6].

For the basic analysis of electromagnetic energy harvesting devices, many authors use a simple load resistor circuit as depicted in Figure 6. According to Priya et al. [9], the inductance of a coil can be neglected for frequencies below 1 kHz. The damping force for a coil with negligible inductive impedance connected to the shown circuit and traveling perpendicular through a magnetic field can be calculated to:

(10) $F_b = Bl_wI = \dfrac{(Bl_w)^2}{R_{coil} + R_{load}}v$

where I is the current flowing in the circuit, R_{coil} is the internal resistance of the electromagnetic coil and R_{load} is the applied load resistance.
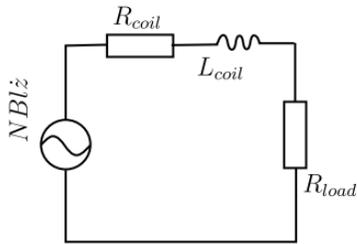
Figure 6: Basic Load-Resistor Circuit

Due to this electro-mechanical coupling, mechanical energy can be transduced to electrical energy. In the first approximation, an electromagnetic damper can be modeled as a viscous damping element. It furthermore has the ability to quickly change its damping constant by altering the load resistor applied in the circuit. The achievable electrical power output is dependent on the size of the load resistor, since only the power generated in the load resistor could theoretically be harvested. A large load resistor decreases the current flowing in the circuit and therefore decreases the achievable damping force. However, the energy conversion efficiency grows when larger load resistors are used, since a larger fraction of the total power is then generated over the load resistor. The maximum power transfer theorem suggests that the most power is extracted from the vibration when the load resistance is chosen to be as large as the internal resistance.

In the context of the „smart spring" damping approach, a linear electromagnetic damper is applied in the secondary load path of the structure. As previously shown, numerical studies showed that most of the energy dissipation takes place in the secondary load path. Furthermore it was explained, that linear electromagnetic dampers increase their energy conversion efficiency when the applied load

resistor is comparably large, thus limiting the possible damping force and equally the damping constant. The „smart spring" mechanism is, therefore, optimized to amplify the damping constant of the electromagnetic damper, thus resulting in a mechanism that offers both high forces and high conversion efficiencies.

5. APPLICATION OF THE „SMART SPRING" DAMPER AS A LEAD LAG DAMPER IN HELICOPTERS

Chapter 3 introduced the idea of using a damping approach based on the „smart spring" with SSDI analogous control. This concept is now applied and integrated into a very simplified model for the lead-lag motion of a helicopter blade, for the sake of demonstration of the principle.

De Jong et al. [10] analyzed the feasibility of harvesting energy from the lead lag motion with a piezo-stack actuator. They mounted the stack to the load-carrying rod of a state-of-the-art hydraulic damper for the lead-lag damping application. The hydraulic damper used has a strongly nonlinear force-velocity progression. The damping force first grows quickly until a velocity of 0,02 m/s (to a value of approximately 9000 N) and remains relatively constant for higher velocities. The authors created a model that considers only the in-plane rigid lagging motion and found out that in fact this simple model agrees well with experimental data provided by Agusta Westland (AW). Moreover, they found out that the lead-lag motion is predominantly excited in the rotor rotation frequency (1/rev). Simulations performed by the authors also show that the proposed design was able to harvest up to $5\ W$ in 130 kn forward flight condition when the largest possible stack was used ($1.5\ cm^2$ x $25\ cm$) with an SSHI (Solid Switch Harvesting on Inductor) control algorithm. In this condition, damper velocities of up to 0,045 m/s were observed.

Building up on this previous work, a numerical model based on the schematic displayed in Figure 7 was created. In the model, the helicopter has a constant rotor speed ω_1 . The blade is modeled as a mass having a moment of inertia J about the rotation axis. No other degree of freedom or any coupling effects are taken into consideration. When the blade is disturbed and a displacement φ is present, the centrifugal force acts on the mass and creates a restoring moment. This restoring moment is modeled with the equivalent stiffness k_{eqv}. The „smart spring" damping assembly is displayed with the mass m_2, the stiffness k_2, the parasitic damping b_1, and the electromagnetic damping b_2. Furthermore, the nonlinear hydraulic damper introduced beforehand is displayed as b_3.
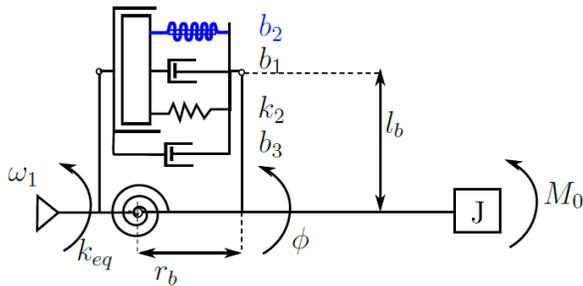
Figure 7: Simplified model of the lead lag motion with integrated „smart spring" damping element.

Table 1: Model Data for the lead lag damper „smart spring" model, partially copied from [8]

f_1	$4.18\ Hz$	k_2	$50\ kN/m$
l_b	$0.25\ m$	ζ_1	0.02
r_b	$0.254\ m$	R_{load}	$15\ R_{wire}$
J	$2387\ kgm^2$	M_0	$10.7e3\ Nm$
k_{eq}	$1.44e5\ N/rad$	n_{coils}	6
m_2	$1\ kg$	C	$20\ mF$

The first simulations performed were targeted to recreate the simulation results of de Jong et al. Thus, the stiffness and damping of the „smart spring" was chosen to be insignificantly small

and the clamping mechanism was activated for the whole simulation time. Therefore only the hydraulic damper contributes significantly to the overall structure and the influence of the „smart spring" is negligible. These simulations performed were able to recreate the results by de Jong et al.

For the subsequent simulations, the „smart spring" was introduced as an additional lead lag damper. The achievable harvested energy is directly proportional to the amount of damping induced by the „smart spring". There are two ways to increase the induced equivalent damping as indicated by equations (5) and (8). Firstly, the stiffness k_2 of the secondary load path can be increased, thereby increasing the force of the spring at a given displacement. Secondly, the displacement itself can be increased by lowering the damping ζ_2 of the secondary load path. It is important to note, that the maximum spring force F_{k2} is limited by the maximum clamping force of the friction based piezoelectric clamp mechanism. No experimental data on the clamping mechanism developed at Carleton University has been generated yet. Therefore, the force is limited to $500\ N$ in the following simulations. State of the art piezoelectric clamping mechanisms were reported to allow loading up to this force level [11]. The stiffness k_2 and damping ζ_2 were, therefore, chosen to result into a maximum spring force of $F_{k2} = 500\ N$. In order to not influence the total damping forces involved in the lead lag motion of the blade, the force of the conventional hydraulic damping element b_3 was then reduced by 8% to $8500\ N$. Figure 8 (top) shows the simulated total damping forces both for the regular hydraulic damper and for the combination including the „smart spring" damper. In steady state, the total forces differ by less than 1%. It is then preliminary concluded, that the integration of the „smart spring" does not alter the stability of the system in any

meaningful way. Figure 8 (bottom) displays the harvested energy from the system. Consider the blue plot first, which was generated using the load resistor circuit displayed in Figure 6. It shows very distinct power peaks with a maximum value of approximately $130\,W$ in steady state. The power peaks are very narrow, because the electrical energy is predominantly generated during the inversion of the secondary load path. In steady state, a mean power of $10\,W$ is generated with an energy conversion efficiency of $80\,\%$.
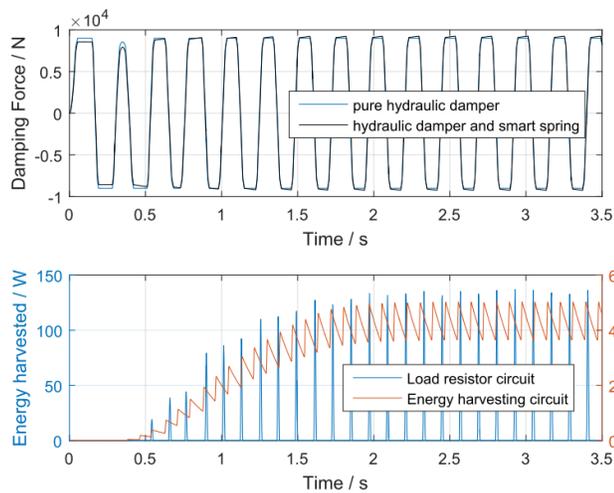
Figure 8: (Top) Total damping force of the conventional hydraulic damper in comparison to the combined hydraulic and „smart spring" damper (Bottom) Energy Harvested when using a load resistor circuit and a basic energy harvesting circuit

In order to utilize this generated energy for any productive use, a power conditioning circuit that offers a stable power supply has to be applied. In this work, the basic energy harvesting circuit displayed in Figure 9 was applied to the electromagnetic damper. The circuit consists of a rectifier and a capacitor that effectively smoothen the signal. The red plot displayed in Figure 8 (bottom) shows the power over the load resistor build into the energy harvesting circuit. In steady-state a relatively continuous power supply of $4.5\,W \pm 0.5\,W$ can be used in the load

resistor. The energy harvesting circuit was, therefore, shown to offer a stable power source. However, the energy conversion efficiency was reduced considerably when compared to that of the simple load resistor circuit.
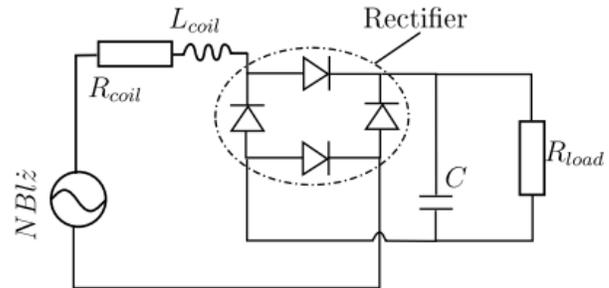
Figure 9: Basic Energy Harvesting Circuit

6. SUMMARY

In this paper, an idea for an electromagnetic energy harvester based on the „smart spring" concept was presented. The modeled device consisted of a piezoelectric clamping mechanism, which can engage and disengage a secondary load path to an internally oscillating mass. A control algorithm taken from the analogy between the „smart spring" and a set of nonlinear vibration control algorithms generally called Synchronized Switch Damping (SSD) was applied to the device. The motion amplitude of the mass in the secondary load path was constrained by a damper. Simulations showed, that the magnitude of the damping coefficient provided by a smart spring can be greatly increased, achieving relatively large equivalent damping constants even with the introduction of a small damper. In this work, the damper was integrated as an electromagnetic damper. The electro-mechanical coupling of the electromagnetic damper allows to transduce the energy of the damping process to useful, electrical, energy.

The concept was then applied to a basic rigid motion lead-lag model of a helicopter blade. The

„smart spring" damper was integrated in parallel to the conventional lead-lag damper and it was designed to account for 5% of the total lead-lag damping force. The simulations showed that a maximum mean power of $10\,W$ can be generated in an $130\,kn$ forward-flight condition. Furthermore, the stability relevant total damping forces were altered by less than 1%.

Future developments should concentrate on experimental studies targeted to validate the concept of using the „smart spring" damper with SSD analogous control algorithms. The basic concept would greatly benefit from new advances in piezoelectric clamping devices that would allow much larger clamping forces. This is because the achievable power output is proportional to the total damping induced by the „smart spring" damper. Furthermore, the concept would also benefit from a motion amplification of the damper displacement, for example based on a mechanical linkage element. This is because increased damper velocities also increase the potential power output. Lastly, in depth research has to be carried out to create a more efficient circuit that fully utilizes the potentially high energy conversion efficiencies of the concept.

7. ACKNOWLEDGEMENTS

8. LITERATURE

1. **Nitzsche, F., Grewal, A., Zimcik, D.** *Structural component having means for cyclically varying its stiffness to control vibrations - „smart spring". EP--996570--B1* Europa, 2001.

2. **Richard, C., Guyoma, D., Audigier, D., Bassaler, H.** *Enhanced semi-passive damping using continuous switching of a piezoelectric device on an inductor.*

3. **Viera, Wander, Nitzsche, F., Carlos de Marqui Junior.** *On the use of synchronized switch damping strategies for the mechanical smart-spring system.* 2015. Currently under review.

4. **Nitzsche, F., Douglas Assuncao, Carlos de Marqui Junior.** *Aeroelastic control of non-rotating and rotating wings using the dynamic stifness modulation via piezoelecrtic actuators.* s.l. : Journal of intelligent Material Systems and Structures, 2015.

5. **Lei Zuo, Brian Scully, Jurgen Shestani, and Yu Zhou.** *Design and characterization of an electromagnetic energy harvester for vehicle suspensions.* s.l. : Smart Materials and Structures, 19(4):045003, 2010.

6. **Zhang, Pei Sheng.** *Design of Electromagnetic Shock Absorbers for Energy Harvesting.* Stony Brook University : Masters Thesis, 2010.

7. **Songye Zhu, Wen-ai Shen, and You-lin Xu.** *Linear electromagnetic devices for vibration damping and energy harvesting: modeling and testing.* s.l. : Engineering Structures 14:198-212, 2012.

8. **Manoli, Dirk Spreemann and Yiannos.** *Electromagnetic vibration energy harvesting devices: Architectures, design, modeling and*

optimization. s.l. : Springer Science & Business Media, 2012.

9. **Inmam, Shashank Priya and Daniel J.** *Energy harvesting technologies.* s.l. : Springer, 2009.

10. **Pieter H de Jong, Andre de Boer, Richard Loendersloot, and Peter JM van der.** *Power harvesting in a helicopter rotor using a piezo stack in the lag damper.* s.l. : Journal of intelligent material systems and structures, 24(11):1392-1404,, 2013.

11. **Quanfang Chen, Da-Jeng Yao, Greg P Carman, et al.** *Mesoscale actuator device: micro interlocking mechanism to transfer macro load.* s.l. : Sensors and Actuators A:Physical, 73(1):30-36, 1999.